



Conference on ENTERprise Information Systems / International Conference on Project
MANAGEMENT / Conference on Health and Social Care Information Systems and Technologies,
CENTERIS / ProjMAN / HCist 2016, October 5-7, 2016

Potential of C-Band SAR Interferometry for Dam Monitoring

Joaquim J. Sousa^{a*}, Antonio M. Ruiz^{b,c,d}, Matúš Bakoň^e, Milan Lazecky^f, Ivana
Hlaváčová^g, Glória Patrício^{h,i}, J. Manuel Delgado^{d,j} and Daniele Perissin^k

^aUTAD, Vila Real and INESC-TEC (formerly INESC Porto), Portugal

^bDpto. Ingeniería Cartográfica, Geodésica y Fotogrametría, Univ. Jaén, EPSJ, Campus Las Lagunillas s/n, Edif. A3, 23071 Jaén, Spain

^cCentro de Estudios Avanzados en Ciencias de la Tierra CEACTierra, Universidad de Jaén, Spain

^dGrupo de investigación Microgeodesia Jaén, Universidad de Jaén, Spain

^eDepartment of Theoretical Geodesy, Slovak University of Technology, Radlinskeho 11, 810 05 Bratislava, Slovakia

^fIT4Innovations, VSB-TU Ostrava, Czech Republic

^gCzech Technical University in Prague, Faculty of Civil Engineering, Thákurova 7, 166 29 Praha 6, Czech Republic

^hInstituto Politécnico da Guarda, Av. Dr. Francisco Sá Carneiro n°50, 6300-559 Guarda, Portugal

ⁱDepartamento de Geociências, Ambiente e Ordenamento do Território, Faculdade de Ciências, Universidade do Porto, Portugal

^jProgressive Systems Srl, Rome, Italy

^kSchool of Civil Engineering, Purdue University, 550 Stadium Mall Drive, West Lafayette, IN47907, Office: HAMP 4106, USA

Abstract

Despite the recent popularity achieved by the modern X-band SAR sensors, mainly due to their high spatial resolutions which enable the detection of deformation components impossible so far, such as thermal expansion, SAR C-band sensors continue to be of great utility and with a great future in the deformation monitoring field, namely for critical structure monitoring, such as dams. The new ESA missions (Sentinel-1A and 1B) and the extension of the Canadian Radarsat mission corroborate this finding. In this paper the possibility of using spaceborne SAR sensors for dam monitoring is addressed in terms of feasibility and applications. The presented results show the potential of C-band sensors for the particular case of dam monitoring and can be helpful to recognize the applicability of new Sentinel-1 data (since 2014) for continuous monitoring of dam deformations.

© 2016 The Authors. Published by Elsevier B.V. This is an open access article under the CC BY-NC-ND license (<http://creativecommons.org/licenses/by-nc-nd/4.0/>).

Peer-review under responsibility of the organizing committee of CENTERIS 2016

Keywords: Dams; Satellite InSAR; Deformation monitoring; C-band SAR

* Corresponding author. Tel.: +351 259 350 357; fax: +351 259 350 480.
E-mail address: jj Sousa@utad.pt

1. Introduction

The perception that structures monitoring has gained a leading role, combined with the certainty that SAR interferometric techniques reached currently a level of maturity that can lead them to an operational level, is the motto of this work. It aims to assess the potential of interferometric techniques in the monitoring and deformation detection of structures, namely the SAR C-band images.

The rapid development of space technologies we have seen in recent decades enabled the development of new earth surface and structures displacement detection techniques from space, with high precision and with unexpected benefits. This progress was only possible thanks to data obtained by the SAR sensors carried on board satellites and to the development of new interferometric processing methods using time series analysis of SAR images^{1,2,3,4,5}.

The finding that some points (pixels in the SAR image) maintained a stable response for large periods of time^{6,7}, provided the launch of the bases for the exploration of interferometric multi-temporal techniques (MT-InSAR), enabling to solve the main limitations of conventional Interferometry (InSAR): first of all, interferograms are affected by temporal and/or geometrical decorrelation; Secondly, the interferometric phase is wrapped, and it may be quite difficult (many times impossible) to unwrap it correctly using a single interferogram; Finally, even if all previous problems are solved, atmospheric artefacts may become fruitless all efforts. MT-InSAR techniques include solutions to some of the mentioned DInSAR limitations. Over the past few years, a number of MT-InSAR algorithms were developed to address the limitations of conventional InSAR, all classified into two categories: Persistent Scatterer Interferometry (PS-InSAR) and Small Baseline (SB). These two techniques were applied to the various data sets used in this work and the results are presented in Section 3.

Recent studies carried out by the authors^{8,9,10,11,12,13} allowed answering the following two key issues relating to the feasibility of using interferometric techniques for structures monitoring:

1. Do most recent interferometric techniques reached a state of maturity and development enabling structures monitoring?
2. What are the main constraints to the application of InSAR techniques for structures monitoring?

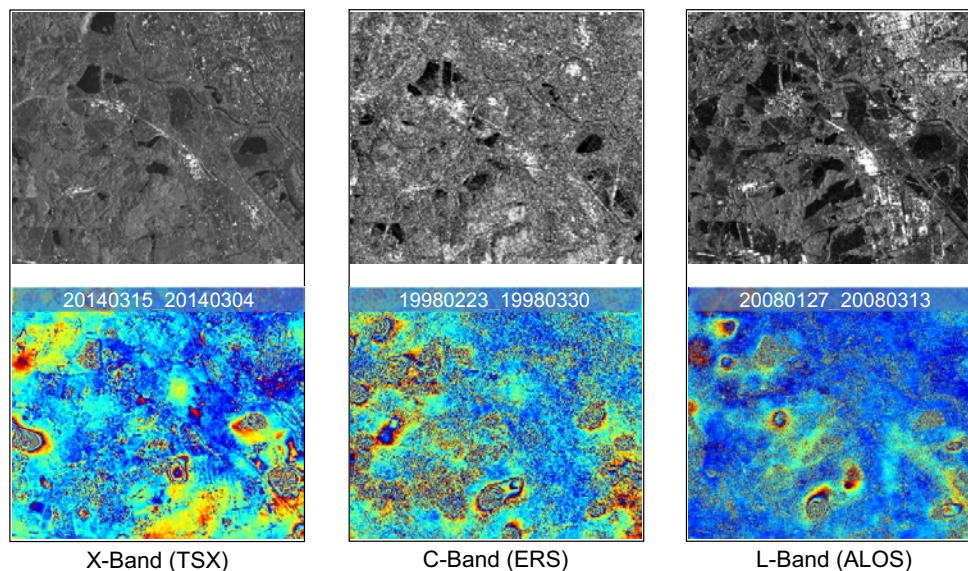


Fig. 1. Comparison between X-, C- and L-band. Top row: amplitude images; Bottom row: interferograms obtained using images acquired in the indicated dates.

The shorter the wavelength is, the more precise the capability of detecting the ground movement. However, the difference of the wavelengths greatly influences the interference property of the ground surface. This is because the

radio wave with shorter wavelength than C-band (~6 cm) hardly penetrates vegetation, e.g., leaves and branches of trees. Therefore observing a forest area by C- or X-band radar (~3 cm), the radio wave is reflected by canopy and cannot reach to the ground. Coherent signals cannot be observed at vegetated areas because leaves swing in the wind or grow up, whereas the signals in urban areas are coherent. On the other hand, a L-band radar (~24 cm), which has a long wavelength, can penetrate the vegetation. For these reasons, but also for the data access policy fostered by the European Space Agency, C-band images appear to be very attractive for structures monitoring, like dams, usually located in non-urbanized areas. The difference between each of the previous radar bands can be perceived in the interferograms and amplitude images presented in Fig. 1.

The several tests carried out using different types of structures have served to establish standard procedures for structures monitoring using interferometric techniques and allowed to conclude that C-band, despite its coarse spatial and temporal resolutions (Sentinel-1 is considerably improved this status), is capable of being used in monitoring major structures, including dams. Obviously, it was soon found that the geometric resolution (0.5-1 m in X-Band) of satellite imagery do not match the size of typical defects, for example in concrete dams (0.01-0.5 m). Problems such as cracking and raveling can therefore not be identified using SAR satellite images; however, the only spaceborne sensor that could possibly contribute to structures inspections by measuring deformations is Synthetic Aperture Radar.

In this paper, MT-InSAR methods are applied to process ERS-1/2, Envisat and Sentinel-1 images for measuring the deformation behavior of several dams, with different construction types and locations.

The paper is structured as follows. Section 2 includes a general description of the interferometric packages using in the processing of SAR data stacks. In Section 3 a general description of each dam studied is followed by the MT-InSAR results. The main conclusions are presented in Section 4.

2. Multi-Temporal Interferometry

Multi-Temporal Interferometry is a group of powerful remote sensing techniques allowing measuring and monitoring displacements of the Earth's surface over time. More generically, it can be said that MT-InSAR is a radar-based technique that belongs to the group of Differential InSAR (DInSAR). Such techniques exploit the radar phase information of at least one pair of complex SAR images acquired over the same region at different times (repeat pass SAR interferometry) and are used to form an interferometric pair (the interferogram). This repeated acquisition of images over a given area is usually performed with the same sensor (or sensors) with identical system characteristics. For a general review of SAR interferometry, the reader is referred to^{14,15}, among others.

Nowadays, several MT-InSAR approaches are available, however they all exploit multiple SAR images acquired over the same area, and appropriate data processing and analysis procedures to separate the displacement component from the other phase components that appear in the interferometric phase. This group of InSAR techniques, focuses in the identification of pixels in the SAR image characterized by small phase noise, which are typically related to two types of reflectors: those where the response to the radar is dominated by a strong reflecting object and remains constant over time (Persistent Scatterer, PS) and those where the response is constant over time, but is due to different small scattering objects (Distributed Scatterers, DS) or SDFP (slowly decorrelating filtered phase), as these specific points are known in StaMPS (Stanford Method for PS/Multi-Temporal InSAR) packages^{1,16}. The SARROZ¹⁷ interferometric package was also used in this work and both packages are summarized in the following subsections.

2.1. StaMPS Package

One of the main characteristics of StaMPS is the fact that the PS selection uses phase characteristics, which is suitable to find low-amplitude natural targets with phase stability that cannot be identified by amplitude-based algorithms. In other words, StaMPS uses phase spatial correlation to identify PS pixels instead of amplitude analysis as in^{3,5,18,19}. An important advantage is that it does not require a prior deformation model. StaMPS evolved to a hybrid method which means that it is based on PS and DS identification, however the main outcomes of all methods remain: the deformation time series; the deformation velocity estimated over the analyzed PS/DS points and the residual topographic error, which represents the difference between the true height of the scattering phase center of a given point and the height of the DEM in this point. This is a key parameter in order to achieve an accurate geocoding.

In StaMPS, the algorithms for PS and SDFP pixels selection are basically the same. However, different interferograms are used. Single master interferograms are used for PS pixel selection, while multiple master interferograms with small baselines (SB) are used for SDFP pixels selection. StaMPS PS pixels selection strategy consists in finding the selection threshold of the probability distribution for each PS candidate. If the converged probability distribution is greater than the selection threshold, the candidate will be initially selected as a PS pixel, otherwise it will be discarded. For the initial topographic estimation, and later on for terrain geocoding a DEM has to be used. After this initial interferometric step, phase unwrapping errors are corrected on the spatial domain using a minimum cost-flow algorithm for sparse data. However, in StaMPS, the non-spatially correlated part in wrapped interferograms is corrected before unwrapping, including the spatially uncorrelated part of the look angle error and the contribution of the master to the spatially uncorrelated part of the signal. Then, the corrected phases are filtered to reduce phase noise before unwrapping²⁰. After Goldstein filtering, the PS pixels are used to form a Delaunay network and their triangle elements are used to find the nearest PS of each grid. The nearest PS pixels of all grids are used to form an unwrapping network.

After phase unwrapping, the phases of PS pixels are already in time series because a common master image is referred for all interferograms. However, for small baseline approach, an inversion of deformation increments from the unwrapped interferograms is necessary as multiple master images are used and the phases are not referenced to the same time. The inversion is implemented using linear equations.

Finally, the unwrapped phases of a single pixel are used to estimate a linear relationship with its spatial perpendicular baselines using least square. After estimating look angle error and master atmosphere, the slave atmosphere is estimated by triangulation of PS or SDFP pixels. The phase on an edge is the difference between the unwrapped phases of two nodes. Because the atmospheric effects are also correlated in space, for each interferogram, the slave atmospheric phases are low-pass filtered in space. This is implemented by sum of neighboring atmospheric phases that are weighted by inverse distances.

The inner workings of this software package are described in more detail in^{1,16,21,22}.

2.2. SARProZ

This interferometric tool package is very versatile, developed in Matlab and is capable to process all available types of SAR images. Initially, this software was developed in order to solve the problem of cross-interferometry (ERS vs. Envisat) using advanced MT-InSAR techniques.

Such problem is strictly related to the physical nature of radar targets and to their capability of being “visible” under different looking angles/illuminating frequencies. Thus, SARProZ was equipped with a module for target characterization and recognition, able to process and extract information also from the amplitude of radar images. As a side-effect, using amplitude time-series the tool became able to deal with temporary targets. Moreover, the recognition of a radar target implies a precise localization, and within SARProZ several techniques for improving the height estimation and the consequent geocoding process were developed²³. The problem of increasing the density of PSs in extra-urban areas was then faced and the Quasi-PS algorithm was studied and implemented²⁴. Currently, SARProZ provides many different options for combining long series of data, and the user can choose which set of interferograms to process and with which techniques. The software includes then some auxiliary functions like classification and change detection. Beside linear deformation trend and height⁵, other parameters can be estimated as azimuth sub-cell position²³ and a constant phase. Parameters can be estimated through the classical PS algorithm as well as through the Quasi-PS one. In the end, APS can be estimated through different algorithms for the graph inversion. All details about this interferometric package can be found in^{24,25} and in the official website (www.SARProZ.com/).

3. Test sites

This section briefly presents the different test areas selected with the aim of achieving the answers to the previously introduced questions but also as function of data availability. Fig. 2 shows the location of the dams used in this work which are summarily described in the following sections. All the presented tests were monitored blindly, i.e. without any reference knowledge, since the goal was the evaluation of C-band feasibility for dam monitoring.



Fig. 2 – Name and location of the dams studied in this work.

3.1. Benínar dam

Benínar dam is located on the Grande de Adra river, in the Andalusian municipality of Benínar, in the Almería province. It was built with loose materials, with distinct profile inclined impervious core, rock fill shoulders and has a height of 87 m and a width of 400 m, the reservoir has a volume of 68,2 hm³. Its catchment area (521 km²) affects the provinces of Granada and Almería on its eastern and western boundaries. Population water supply and irrigation are the main use of this dam. In the MT-InSAR processing of this dam, StaMPS algorithm was used in a set of 22 ERS descending images from 06/06/1992 to 31/10/2000 and 32 Envisat ascending images from 03/12/2002 to 29/06/2010. The results are presented in Fig. 3.

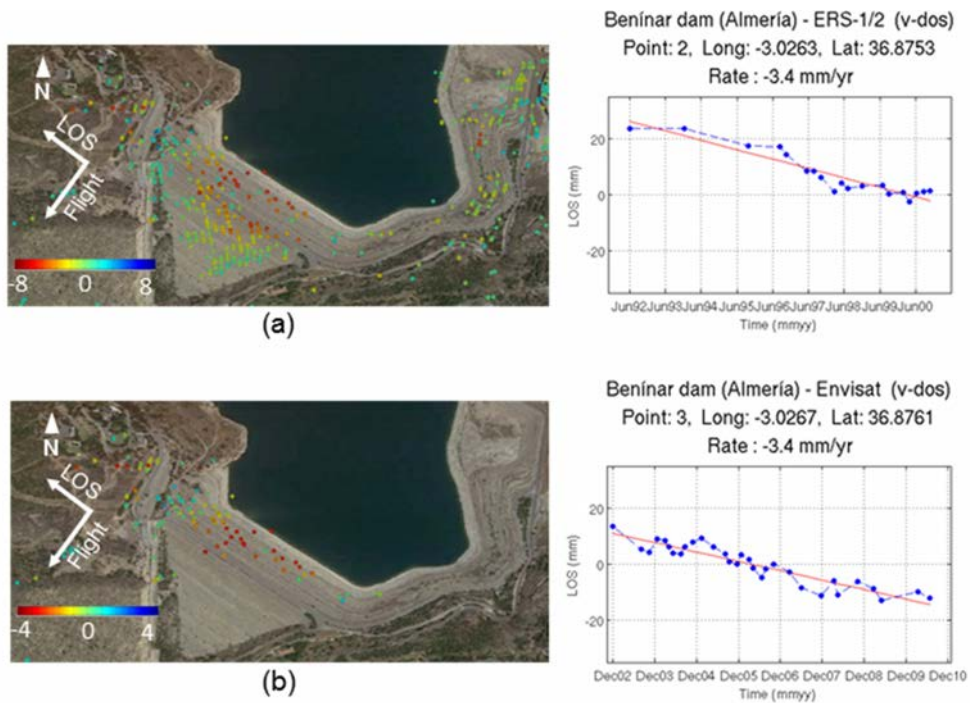


Fig. 3 – StAMPS MT-InSAR mean LOS velocity for Benínar dam with a time-series deformation plot of a point on the top of the dam (a) ERS descending track 8; (b) Envisat ascending track 416.

In both datasets, the dam is defined by several high-intensity stable points, that show some deformation trend in rate of -3 to -4 mm/yr (on the top of the dam) falling to zero deformation on the bottom of the dam. Such movement can be assumed in horizontal direction, perpendicularly to the dam axis, and represents the expected behavior for this type of dam.

3.2. El Limonero dam

The El Limonero dam is located on the outskirts of Málaga city, situated on the Guadalmina river and belongs to the Cuenca Mediterránea Andaluza. The main objective of this dam is the lamination of the avenues of the Guadalmina river, but serves also as a supply source for the city of Málaga. The dam type is loose materials and plant with core curve. It has a crest length of 414 m, a height over foundation of 95 m and a height above the bed of 76 m. In the MT-InSAR processing of this dam, StAMPS algorithm was used in a set of 27 ERS ascending images from 04/10/1992 to 06/09/2000. The results are presented in Fig. 4.

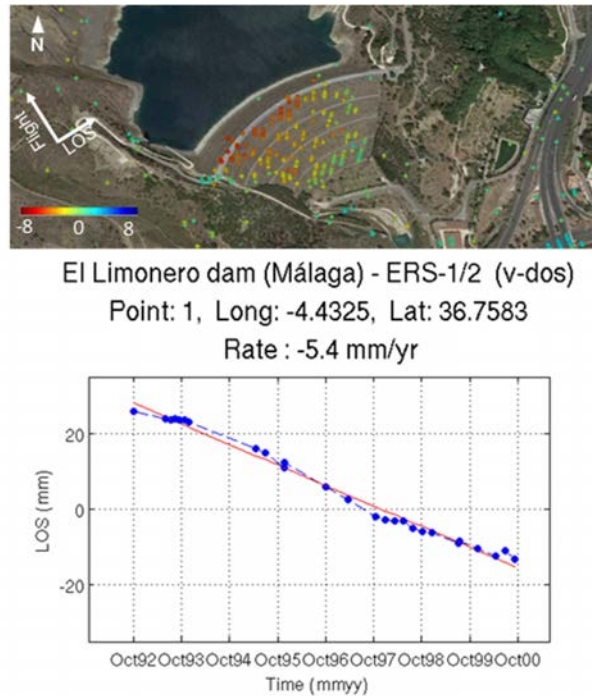


Fig. 4 – StAMPS MT-InSAR mean LOS velocity (left) and a deformation time-series plot for a point on the top of the dam (right) for El Limonero dam (ERS ascending track 230).

Again, the detected movements up to -4 to -5 mm/yr on the top of the dam was expected for this type of dam..

3.3. La Viñuela dam

La Viñuela dam is located on the Guaro river, in the municipality of La Viñuela and controls the waters of the hydrographic network of the region of La Axarquía. It has been built to supply water to the region and to improve the irrigated lands. The basin of the La Viñuela reservoir has an own surface of 119 km², an average yearly rainfall of 893 mm and an average yearly contribution of 25 hm³. The reservoir is made of loose materials (embankment dam) and mixed plant, having a coronation length of 460 m, a foundations height of 96 m and a height over the riverbed of 90 m. In the MT-InSAR processing of this dam, StAMPS algorithm was used in a set of 24 ERS descending images from 05/05/1992 to 28/01/2000 and 27 Envisat ascending images from 21/03/2003 to 01/08/20082. The results are presented in Fig. 5.

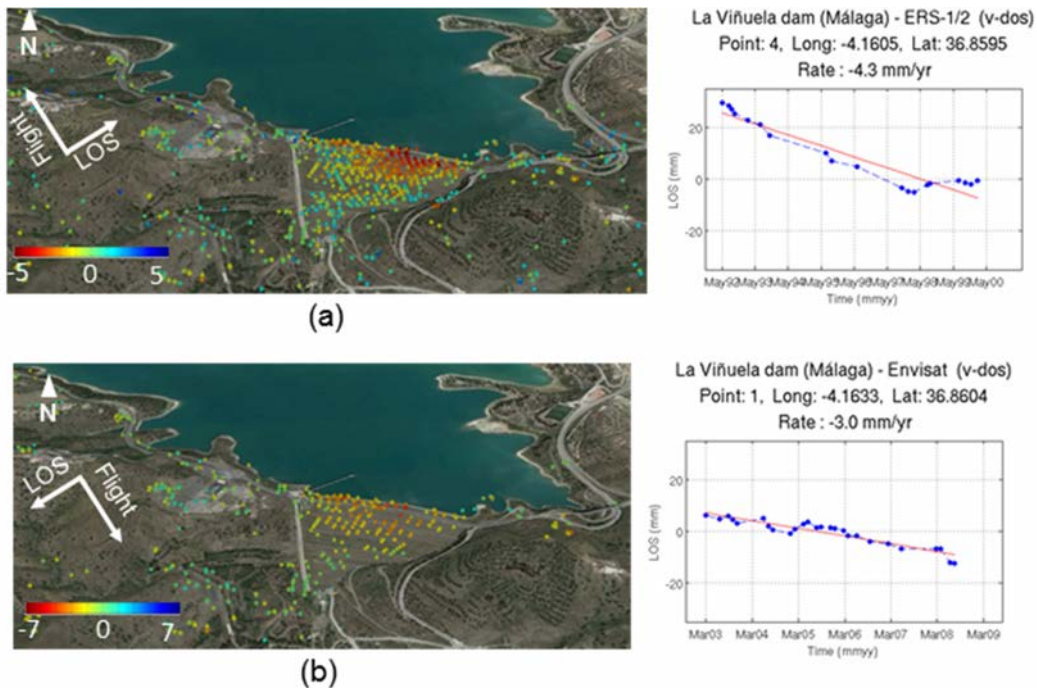


Fig. 5 – StAMPS MT-InSAR mean LOS velocity and one time series plot of a larger deformation for La Viñuela dam: (a) ERS descending track 51; (b) Envisat ascending track 459.

Despite the distinct geometries of both datasets, several PS are found in the dam wall. The behavior of the displacements clearly indicates that the deformation occurs in an expected way due the water pressure.

3.4. Arenoso dam

El Arenoso dam is located in the Arenoso riverbed, a tributary of the Guadalquivir on the right bank, in the Andalusian municipality of Montoro, province of Córdoba and its reservoir has a capacity of 166,97 hm³ and a area of 764,12 ha. The type of dam is loose materials with impervious core, filters and rock fill shoulders. The dam has a maximum height of 80 m, a crest length of 1.481 m and a coronation width of 11,30 m. The construction of the dam increased the water available in the Guadalquivir which affects the economic and social development of the Guadalquivir basin. In the MT-InSAR processing of this dam, SARProZ algorithm was used in a set of 28 Sentinel-1A images from 15/03/2015 to 02/02/2016. The results are presented in Fig. 6.

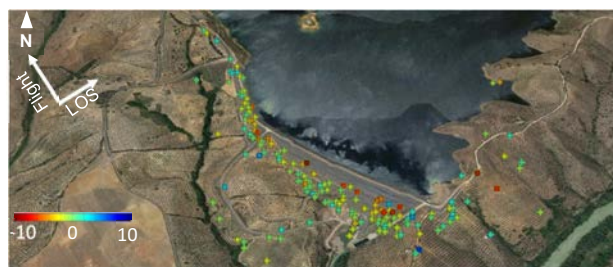


Fig. 6 – SARProZ MT-InSAR results for El Arenoso dam (Sentinel-1A ascending track 74).

Nothing significant can be detected when compared to the previous processing; however this Sentinel-1A dataset allows realizing the added value brought by the C-band sensor on board Sentinel-1A.

3.5. Paradela dam

Applying SARProZ to Envisat images from overlapping ascending tracks 273 (14 images from 10/2002-05/2007) and 44 (16 images from 05/2003-12/2007) using closely corresponding reference point, the results show very similar behavior, however for different PS points. In both datasets the dam is defined by several high-intensity stable points. These stable points are showing some (rather small) deformation trend in rate of not more than 2 mm/yr on the lower part of the dam and up to ~5 mm/yr on the upper part of the dam in satellite LOS. The situation is described in Fig. 7, including graphs of linear deformation estimated at two selected points, located at close positions within datasets of both tracks.

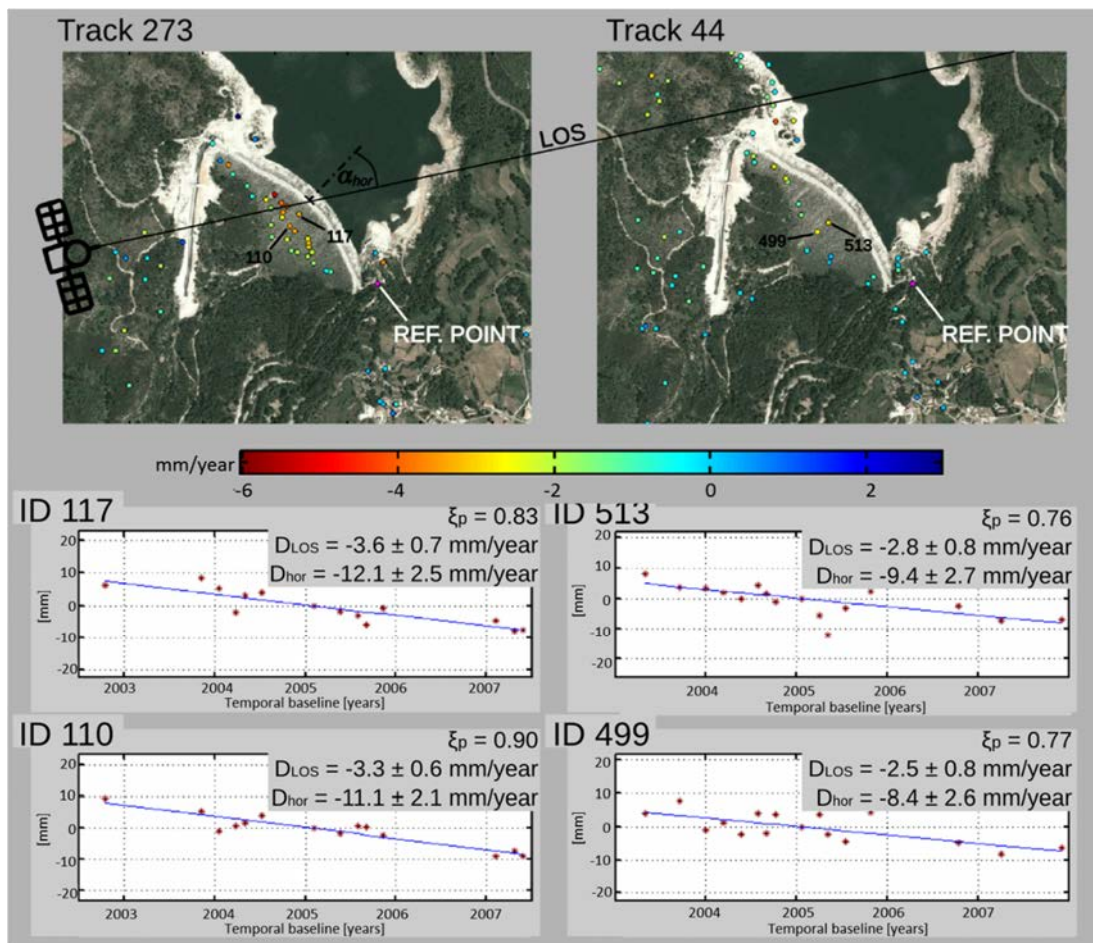


Fig. 7 – (a) Linear LOS deformation trend of Paradela dam estimated using SARProZ MT-InSAR processing of Envisat ASAR data of track 273 (left) and track 44 (right); (b) Deformation time series of marked PS.

3.6. Raiva dam

The Raiva dam is a concrete dam with a length of 200 m, situated in central Portugal, on the Douro river near the Coiço town. The area is monitored using ENVISAT data from two ascending tracks where the orientation of the dam is almost ideal - parallel to the flight direction. Data from 2003-2007 (track 44, 20 scenes) and 2003-2005 (track 316, 16 scenes) were processed. Due to longer spatial and temporal baselines and lower number of scenes, track 316 is less suitable for monitoring; however it has slightly better resolution in the direction perpendicular to the dam construction. The dam is subject to a strong radar layover from both tracks, as the PS points on the top of the dam are closer to the radar than the PS points on the bottom side. The northern part of the dam is not visible by the radar or the PS points were excluded from the processing due to inappropriate quality (coherence). In Fig. 8a (track 44), no significant movement is visible, however in Fig. 8b (track 316), movement of the slope is detected. Note that identified high-quality PS points are different. Within the accuracy of the method, i.e. within few mm, there is nothing happening at the dam. On the slopes, movements are possible, however the point density (or coherence) is low; the results for the two tracks do not verify one another, but they both present stable behavior of the dam.

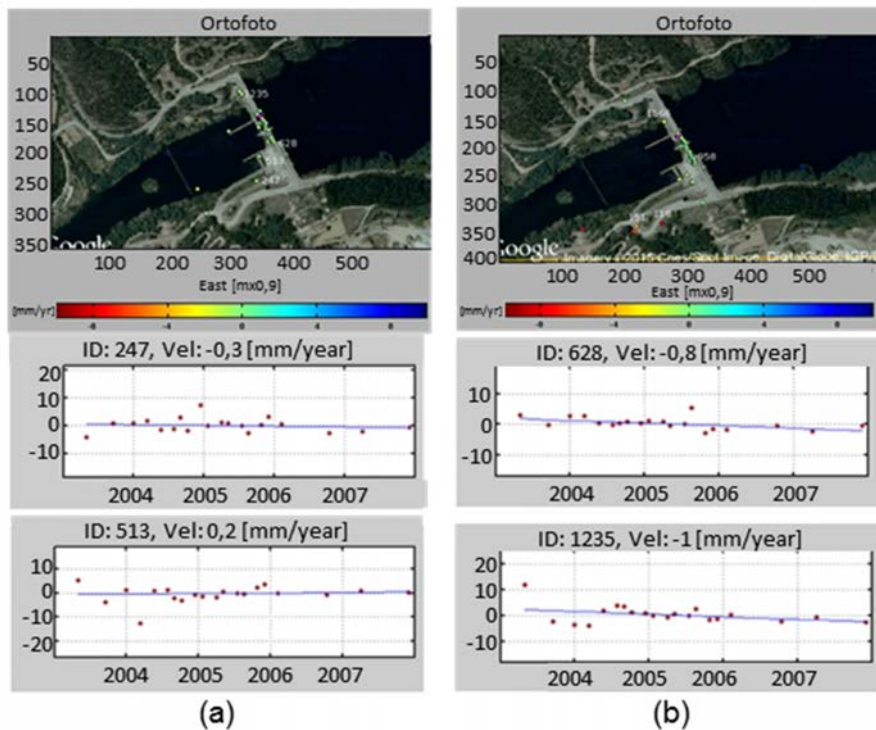


Fig. 8 – Estimated linear deformation with marked distinctive PS points: (a) for track 44; (b) for track 316.

4. Conclusion

In this work we focused on the evaluation of vulnerability of dams affected by terrain movements and proved that structure movements can be observed using satellite-based SAR interferometry techniques using C-band data (ERS, Envisat and Sentinel-1). It was concluded that ERS and Envisat SAR scenes are suitable for structural monitoring, in particular, to determine the overall state of the structure. Using the data collected by the new SAR sensor on board Sentinel-1 satellite, it was possible to conclude that new generation of C-band sensors will allow several benefits in terms of temporal and spatial resolutions but also in the coherence which will be reflected in a significant increase of PS/DS points. InSAR also provides an additional value to optimize estimated subsidence models and potentially

discover unknown dynamics thanks to its high revisit rate (6 days for Sentinel-1A and 1B) which would allow a near real-time analysis possibility and unique opportunity of precise spatial information (around millimetric sensitivity). Yet an early warning can be achieved only in case of slowly developing changes so that the result of processing several acquired radar acquisitions can infer statistically confident outcomes.

Acknowledgements

This work was partially supported by: (1) European Fund for Regional Progress - FEDER through the project BI/COMPETE/38732/UTAD/2014 entitled “RemotWatch – Alert and Monitoring System for Physical Structures”; (2) PRX14/00340 and ESP2006-28463 projects from Ministerio de Ciencia e Innovación (Spain); (3) UJA2015/08/05 and CEACTierra projects from University of Jaén (Spain); (4) RNM-282 research group from the Junta de Andalucía (Spain); (5) Ministry of Education, Youth and Sports from the National Programme of Sustainability (NPU II) project “IT4Innovations excellence in science - LQ1602” and from the Large Infrastructures for Research, Experimental Development and Innovations project “IT4Innovations National Supercomputing Center – LM2015070” and (6) Slovak Grant Agency VEGA under projects No. 1/0714/15 and 1/0462/16. ERS and Envisat data were provided by ESA within the 28760, 7629 and 13537 C1.P projects and Sentinel-1A data were provided by ESA under free, full and open data policy adopted for the Copernicus programme. Data have been processed by StaMPS and SARProZ (Copyright (c) 2009-2016 Daniele Perissin) and visualised in Matlab® using Google Maps™ and Google Earth™.

References

1. Hooper A, Segall P, Zebker H. *Persistent scatterer InSAR for crustal deformation analysis, with application to Volcán Alcedo, Galápagos*. J Geophys Res 112:B07407, 2007. doi:10.1029/2006JB004763.
2. van der Kooij, M., W. Hughes, S. Sato, and V. Poncos. *Coherent target monitoring at high spatial density: Examples of validation results*. Eur. Space Agency Spec. Publ., SP-610, 2006.
3. Kamps, B.M. *Radar Interferometry: Persistent Scatterer Technique*. Springer, Dordrecht, The Netherlands, 2006.
4. Berardino, P., Fornaro, G., Lanari, R., Sansosti, E. *A new algorithm for surface deformation monitoring based on small baseline differential SAR interferograms*. IEEE Transactions on Geoscience and Remote Sensing, 40(11), 2375 – 83, 2002.
5. Ferretti, A., Prati, C., Rocca, F. *Permanent scatterers in SAR interferometry*. IEEE TGRS 39 (1), 8–20, 2001.
6. Usai, S. *The use of man-made features for long time scale INSAR*. Geoscience and Remote Sensing, 1997. IGARSS '97. Remote Sensing - A Scientific Vision for Sustainable Development., 1997 IEEE International, 4, 1542-1544, ISBN: 0-7803-3836-7.
7. Usai, S. and R. Hanssen. *Long time scale INSAR by means of high coherence features*. Third ERS Symposium on Space at the service of our Environment, held in Florence, Italy, 14-21 March, 1997. Compiled by T.-D. Guyenne and D. Danesy. European Space Agency, p. 225.
8. Lazecky, M.; Hlavacova, I.; Bakon, M.; Sousa, J.J., Perissin, D.; Patricio, G. *Bridge Displacements Monitoring using Space-Borne SAR Interferometry*. IEEE Journal of Selected Topics in Applied Earth Observations and Remote Sensing, 2016 (in press).
9. Lazecky, M.; Hlavacova, I.; Bakon, M.; Papco, J.; Kolomaznik, J.; Sousa, J.J. *Satellite InSAR Applicability for Monitoring Bridge Deformations*. 8th International Conference on Bridge Maintenance, Safety and Management, June 26 - 30, 2016, Foz do Iguaçu, Brazil (accepted).
10. Lazecky, M.; Bakon, M.; Sousa, J. J.; Perissin, D.; Hlavacova, I.; Patricio, G.; Rapant, P.; Real, N. and Papco, J. *Potential of Multi-Temporal InSAR Techniques for Structural Health Monitoring*. FRINGE 2015 – Advances in the Science and Applications of SAR Interferometry and Sentinel-1 InSAR Workshop, 23-27 March 2015, ESA-ESRIN (Frascati, Italy). ESA, CD-ROM SP-731. ISBN: 978-92-9221-295; ISSN: 1609-042X.
11. Lazecky, Milan; Sousa, J. J.; Hlavacova, Ivana; Comut, Fatma C.; Refice, Alberto; Papco, Juraj; Ustun, Aydin; Perissin, Daniele; Dobes, Pavel; Ruiz-Armenteros, Antonio M.; Jirankova, Eva; Rapant, Petr. *Potential of Satellite-borne InSAR Monitoring System for Risk Management of Infrastructure Damage due to Terrain Displacements*. Mapping Urban Areas from Space Conference. 4 and 5 November 2015, Rome Italy.
12. Sousa, J.J., Hlaváčová, I., Matúš, B., Lazecký, M., Patrício, G., Guimarães, P., Ruiz, A.M., Bastos, L, Sousa, A. and Bento, R. *Potential of Multi-Temporal InSAR Techniques for Bridges and Dams Monitoring*. Journal of Procedia Technology, Volume 16, 2014, Pages 834–841, doi:10.1016/j.protec.2014.10.033, 2014.
13. Sousa, J.J. and Bastos, L. *Multi-temporal SAR interferometry reveals acceleration of bridge sinking before collapse*. Nat. Hazards Earth Syst. Sci., 13, 1–9, doi:10.5194/nhess-13-659-2013.
14. Bamler, R., Hartl, P. *Synthetic aperture radar interferometry*. Inverse Probl. 14, R1–R54, 1998.
15. Rosen, P.A., Hensley, S., Joughin, I.R., Li, F.K., Madsen, S.N., Rodriguez, E., Goldstein, R.M. *Synthetic aperture radar interferometry*. Proc. IEEE 88 (3), 333–382, 2000.
16. Hooper A. *A multi-temporal InSAR method incorporating both persistent scatterer and small baseline approaches*. Geophys Res Lett 35:L16302. doi:10.1029/2008GL034654, 2008.
17. Perissin, D., Wang, Z., Wang, T. *The SARProZ InSAR tool for urban subsidence/manmade structure stability monitoring in China*. In: Proceedings of 34th International Symposium for Remote Sensing of the Environment (ISRSE), Sydney 2001.

18. Colesanti, C., Wasowski, J. *Investigating landslides with space-borne Synthetic Aperture Radar (SAR) interferometry*. Eng. Geol. 88 (3), 173–199, 2006.
19. Ketelaar, V.B.H.G. *Satellite Radar Interferometry, Subsidence Monitoring Techniques*. Springer, 2009. ISBN-13: 978-1402094279.
20. Goldstein, R.M. & Werner, C.L.. *Radar interferogram filtering for geophysical applications*. Geophys. Res. Lett., 25, 4035-4038, 1998.
21. Sousa J, Ruiz A, Hanssen R, Bastos L, Gil A, Galindo-Zaldívar J, Sanz de Galdeano C. *PS-InSAR processing methodologies in the detection of field surface deformation study of the Granada Basin (Central Betic Cordilleras, Southern Spain)*. J Geodyn 49:181–189. doi:10.1016/j.jog.2009.12.002, 2010.
22. Sousa J, Hooper A, Hanssen R, Bastos L, Ruiz A. *Persistent scatterer InSAR: a comparison of methodologies based on a model of temporal deformation vs. spatial correlation selection criteria*. Remote Sens Environ 115(10):2652–2663, 2011.
23. D. Perissin and F. Rocca. *High accuracy urban DEM using permanent scatterers*, IEEE Trans. Geosci. Remote Sens., vol. 44, no. 11, pp. 3338–3347, Nov. 2006.
24. Perissin, D. & Wang, T. *Repeat-Pass SAR Interferometry with Partially Coherent Targets*. IEEE T. Geoscience and Remote Sensing, 50, 271-280, 2012.
25. D. Perissin, Z. Wang, T. Wang. *The SARProZ InSAR tool for urban subsidence/manmade structure stability monitoring in China*. Proc. of ISRSE 2010, Sidney, Australia, 10-15 April 2011.